ORIGINAL PAPER

Recent and historical tsunami deposits from Lake Tokotan, eastern Hokkaido, Japan, inferred from nondestructive, grain size, and radioactive cesium analyses

Tetsuya Shinozaki[1,2] · Yuki Sawai[2] · Kazumi Ito[2] · Junko Hara[2] · Dan Matsumoto[2] · Koichiro Tanigawa[2] · Jessica E. Pilarczyk[3,4]

Abstract

Geological evidence of recent tsunamis from sediment samples collected from Lake Tokotan, a coastal lagoon in eastern Hokkaido, northern Japan, was detected using computed tomography (CT) and soft X-ray images, grain size, and radionuclide profiles. Initial field observations revealed that sediments had no discernable sedimentary structures at the top of the core. However, results of CT imaging, soft X-ray, and grain size analyses show evidence for three invisible sand layers that are intercalated with mud layers. These sand layers exhibit trends of landward fining and thinning. Furthermore, the distribution of sand layers was limited to the center and seaward parts of the lake. Vertical profiles of cesium and lead concentrations in combination with recent eyewitness accounts indicated that these sand layers are correlated with the 1973 Nemuro-oki, 1960 Chilean, and 1952 Tokachi-oki tsunami events. The deeper part of the sediment cores includes three volcanic ash layers and three prehistoric coarse sand layers. The prehistoric layers are correlated with unusually large tsunamis that were geologically identified in previous studies from eastern Hokkaido. These findings suggest that nondestructive techniques, in combination with radionuclide analysis, allow for detection of frequent but faint tsunami deposits. This technique allows for an improved understanding of the history of tsunami inundation in Lake Tokotan and of other locations for which stratigraphic evidence for faint tsunamis layers is not readily apparent from field assessments.

✉ Tetsuya Shinozaki
   shinozaki@ied.tsukuba.ac.jp

1   Center for Research in Isotopes and Environmental Dynamics (CRiED), University of Tsukuba, Tennodai 1-1-1, Tsukuba, Ibaraki 305-8577, Japan

2   Geological Survey of Japan, National Institute of Advanced Industrial Science and Technology (AIST), Higashi 1-1-1-C7, Tsukuba, Ibaraki 305-8567, Japan

3   Department of Earth Sciences, Centre for Natural Hazards Research, Simon Fraser University, 8888 University Dr., Burnaby, BC V5A 1S6, Canada

4   Division of Marine Science, School of Ocean Science and Technology, University of Southern Mississippi, 1020 Balch Blvd., Stennis Space Center, MS 39529-9904, USA

Abbreviations

CT   Computed tomography
Ta-a   Tarumai-a
Ko-c2   Komagatake-c2
Ta-b   Tarumai-b

1 Introduction

Tsunami waves erode, transport, and redeposit offshore sediments and coastal sediments on land. The redeposited sediments (tsunami deposit) are often preserved in low-energy coastal lowland areas such as lakes, marshes, and swamps (Goff et al. 2012). Buried tsunami deposits are usually first recognized as coarse sedimentary layers that are intercalated with muddy or organic-rich sediments (Cisternas et al. 2005; Jankaew et al. 2008; Fujino et al. 2009; Sawai et al. 2012). However, tsunami events do not always leave a sedimentary deposit behind because the wave action can be too weak to transport and leave clear and visible sandy deposits on the coast (Goto et al. 2011). Weaker tsunamis often go undetected in the stratigraphic record because they do not leave a thick enough deposit that can be observed in field investigations. This study assesses whether faint event deposits that are not stratigraphically recognizable by observation in field investigations can be detected using a combination of computed tomography (CT), soft X-ray images, grain size and geochemical analyses, and cesium and lead dating on lake bottom sediment of Lake Tokotan, eastern Hokkaido.

The Pacific coast of eastern Hokkaido, northern Japan, has been struck frequently by large tsunamis, both in prehistoric and historical times. Geological records have revealed that, in prehistoric times, recurrent tsunami events generated by multi-segment earthquakes rupturing the offshore segments of Tokachi (Tokachi-oki) and Nemuro (Nemuro-oki) along the Kuril Trench left a series of extensive sand sheets on the coastal lowlands (e.g., Nanayama et al. 2003; Sawai et al. 2009 and references therein). By contrast, in historical and recent times (the last 100 years), tsunamis generated by single-segment earthquakes (e.g., 1952 CE Tokachi-oki) damaged the Pacific coast of eastern Hokkaido (Central Meteorological Agency 1953) (Table 1). Damage and areas inundated by recent tsunamis have been well recorded (details in Sect. 2.2), but no geological records of these events have previously been recognized.

2 Study area

2.1 Geomorphology

Lake Tokotan, a small coastal lake (about 600×450 m, 1.0–2.0 m water depth) located in eastern Hokkaido, faces the Kuril Trench (Fig. 1). The lake, which is situated approximately 300 m inland from the shoreline (Fig. 1d), is isolated from the sea by a sand barrier (max. 5 m high above the present sea level, Fig. 1e). It has narrow drainage (Tokotan River), but it does not receive major river inflow (Fig. 1d). Lake Tokotan is characterized by freshwater with no marine inputs because of its isolation from the sea. Lowland areas around the lake are surrounded by Pleistocene marine terraces that reach a height of approximately 40–60 m in height (Okumura 1996) (Fig. 1d).

Table 1 Tsunami and storm history at Akkeshi. Magnitudes of earthquakes were referred from Tanioka et al. (2004), The Japan Meteorological Agency (1974), Barrientos and Ward (1990), MacInnes et al. (2010), Hirata et al. (2004), and Utsu (1999)

| Tsunami source (Mw: moment magnitude, M: magnitude)	Date of tsunami inundation	Tsunami height at Tokotan
Tsunamis		
Tokachi-oki (Mw 8.0)	September 26, 2003	1.9–3.1 m tsunami wave (Tanioka et al. 2004)
Nemuro-oki (Mw 7.8)	June 17, 1973	2–2.5 m run-up height (The Japan Meteorological Agency 1974)
Concepcion, Chile (Mw 9.5)	May 22, 1960	1.8 m above the mean tidal level (The Japan Meteorological Agency 1961)
Kamchatka, Russia (Mw 8.8–9.0)	November 4, 1952	No inundation records around Tokotan
Tokachi-oki (Mw 8.1)	March 4, 1952	2 m tsunami height (Sapporo District Central Meteorological Observatory 1954)
Tokachi-oki (M 8.0)	April 25, 1843	4–5 m tsunami height (Hatori 1984)
Area of devastation	Date of storm attacked	Remarks
Storms		
Eastern Hokkaido	December 16, 2014	Passed off Nemuro, no inundation records around Tokotan (Saruwatari et al. 2015)
Eastern Hokkaido	September 12, 1879	1.5 m above sea level (Akkeshi Town 2007)
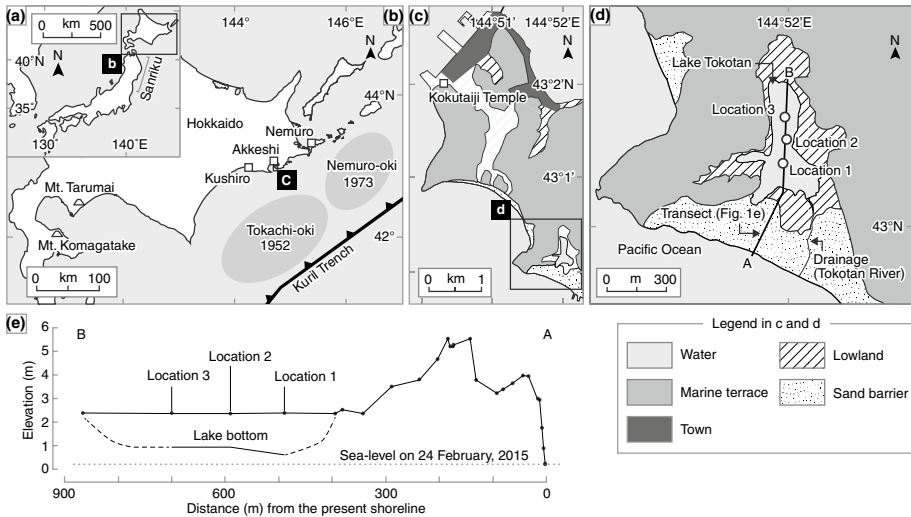
Fig. 1 Location map of the study area. **a** Map of Japan. **b** Map of Hokkaido, northern Japan, showing the rupture area of the 1952 Tokachi-oki (Hirata et al. 2004) and 1973 Nemuro-oki (Nakanishi et al. 2004) earthquakes. **c** Southern part of Akkeshi Town, showing the location of Lake Tokotan and the Kokutaiji Temple. **d** Close-up maps showing sampled locations. A–B is the leveled transect. **e** Topographic profile and the location of sampled points along transect A–B

2.2 Tsunami inundation history

2.2.1 1843 Tokachi-oki earthquake

On April 25, 1843, an earthquake occurred offshore of Tokachi (1843 Tokachi-oki earthquake) (Watanabe 1998). Nikkan-ki, a series of diaries by successive monks from the Kokutaiji Temple (Fig. 1c) at Akkeshi Town, described the event as being characterized by an "unprecedentedly large earthquake and tsunami." According to the written records, stone lanterns and Buddhist statues collapsed outside of the temple gate. The subsequent tsunami inundated areas close to an assembly hall (possibly near the temple), where it was described as appearing like the ocean. The tsunami height was estimated to be 4–5 m (Watanabe 1998). All lodges and homes of the Ainu (native people of Hokkaido) were washed away (Akkeshi Town 2015). These historical descriptions of coastal damage are not from the Tokotan site but from the former central part of Akkeshi (near Kokutaiji Temple; Fig. 1c).

2.2.2 1952 Tokachi-oki earthquake

On May 4, 1952, an earthquake occurred offshore of the Tokachi region (1952 Tokachi-oki earthquake) (Central Meteorological Agency 1953; Inoue 1954) (Fig. 1b). During the years following the earthquake, several research groups visited the Tokotan site and described the damage associated with the earthquake and the ensuing tsunami.

Sapporo District Central Meteorological Observatory (1954) reported that the first tsunami wave arrived about 35 min after the main shock with heights of approximately 5 m above sea level. As the tsunami wave came ashore, its height was reduced to 2 m. The resulting inundation reached approximately 400 m inland of the shoreline. Two deaths, four severe injuries, and 37 collapsed houses were reported. In addition, approximately 100 buildings experienced flooding reaching above/below floor level. Fishing vessels were washed away. Tsunami inundation reported by Sapporo District Central Meteorological Observatory (1954) does not include the area of Lake Tokotan.

A similar study by a group consisting of representatives from the Akkeshi Assembly provided additional details related to coastal damage resulting from the 1952 Tokachi-oki tsunami. The representatives' group visited Tokotan one day after the earthquake and documented the tsunami effects through photographs and eyewitness interviews (Akkeshi Town 2015, Murosaki in personal communication). According to eyewitness accounts, approximately 30 min after the main shock, a tsunami wave tracking from the south reached the village and increased water levels near a narrow inlet connecting Lake Tokotan with the sea. The tsunami wave caused a strong current to flow into the lake along the inlet, causing houses near the inlet to be washed landward into the lake. Photographic evidence taken by a member of the research group, Kyousuke Murosaki, showed that fishing vessels and houses had been transported up to the southern part of the lake by tsunami waves (Fig. 1d). As a direct result of the earthquake, three deaths, 18 severe injuries, and 44 collapsed houses were reported.

2.2.3 1960 Chilean earthquake

In 1960, a tsunami originating from the Chilean subduction zone tracked across the Pacific Ocean and damaged the northeastern Japanese coast. In Hokkaido, Kiritappu marsh, about 20 km east of Tokotan, was inundated by tsunami waves that reached a few hundred meters inland from the shoreline. The tsunami heights in northern Kiritappu were 3.2–3.9 m on the coast. In contrast, the tsunami waves in Tokotan were relatively small (The Japan Meteorological Agency 1961). The local sea level began to fall at approximately 4 AM local time. The sea level then rose, but the highest level was almost equal to that of storms that are typical of the area (The Committee for field investigation of the Chilean tsunami of 1960 1961). The highest wave was 1.8 m above the mean tidal level (The Japan Meteorological Agency 1961), but no record can be found reporting inundation damages to the village (The Committee for field investigation of the Chilean tsunami of 1960 1961).

2.2.4 1973 Nemuro-oki earthquake

An earthquake occurred offshore of the Nemuro Peninsula on June 17, 1973 (Fig. 1b). The first consequent tsunami wave struck the Tokotan site approximately 30 min later. Tsunami waves reached almost to the top of the coastal breakwater (about 3 m higher than the sea level at the time of tsunami arrival), but did not inundate the coastal village behind it. Nevertheless, the tsunami waves were funneled into the Tokotan River, destroying coastal pilings (Bureau for Ports and Harbours et al. 1973). The tsunami run-up height was estimated as approximately 2–2.5 m based on watermarks preserved on coastal pilings (The Japan Meteorological Agency 1974).

2.2.5 2003 Tokachi-oki earthquake

On September 26, 2003, a large earthquake struck the Tokachi region (Yamanaka and Kikuchi 2003). The resulting tsunami propagated along the Pacific coast not only toward Hokkaido, but also toward Sanriku (Fig. 1a) (Hirata et al. 2004). Immediately after the earthquake, tsunami heights along the coast were measured at various locations including Lake Tokotan. At the Tokotan site, tsunami waves were 1.9–3.1 m high (Tanioka et al. 2004).

2.3 Storm and flooding

The study area, located in eastern Hokkaido, is vulnerable to effects of severe typhoons as a result of their attenuation by the time they reach to Hokkaido (Elsner and Liu 2003). Historical archives in Akkeshi Town include 11 descriptions of "storm" or "flooding" (including "typhoon" and "inundation") that occurred in Akkeshi, Kushiro, or Nemuro between 1808 and 1960 CE (Akkeshi Town 2007). Most notably, a marine inundation event that occurred in 1879 CE represents an extremely severe storms among the recorded events. Although no description of an associated deposit has been found, written records indicate that the storm inundated the Wangetsu area (near Kokutaiji Temple). It reached only about 1.5 m above sea level (Akkeshi Town 2007). In December 2014, a severe storm passed offshore of Nemuro, causing storm surge flooding around the Nemuro area (Saruwatari et al. 2015), but no flooding or inundation was reported at the study site.

3 Geological evidence of historical and prehistoric tsunamis

Along the Pacific coast of Hokkaido, coastal marsh deposits had previously provided evidence for recurrent large tsunamis. Nanayama et al. (2003, 2007) found sand sheets interbedded with peaty deposits beneath coastal marshes. They attributed the sand sheets to large tsunamis based on sedimentary structures, micropaleontology, and the lateral extent of the sand layers. They also proposed a fault model to explain the occurrence of the investigated tsunami deposits, which revealed that a Mw 8.5 earthquake had struck the coastline earlier (Satake et al. 2008). The model was later reexamined and upgraded to Mw 8.8 by Ioki and Tanioka (2016).

The recurrence interval of such a tsunami was first estimated, based mainly on tephrochronology, as approximately 500 years over the past 2500 years (Nanayama et al. 2003). After studies conducted by Nanayama et al. (2003, 2007), Sawai et al. (2009) constrained depositional ages of two historical and 15 prehistoric tsunami deposits from Kiritappu and Mochirippu using dozens of radiocarbon ages. They concluded that the intervals between the unusually large tsunamis average approximately 400 years but range from approximately 100 to 800 years. In addition, Nishimura et al. (2000) found a sand sheet above the Tarumai-a tephra ("Ta-a"; 1739 CE), which has been attributed to a tsunami deposit generated by the 1843 CE Tokachi-oki earthquake.

Paleotsunami studies from Lake Tokotan have been conducted by Nanayama et al. (2001), Sawai (2002), and Shigeno et al. (2007). These reports describe that tsunami deposits generated by the seventeenth century and older earthquakes were confirmed in

lake bottom cores. However, geological evidence for the nineteenth–twenty-first century tsunami events was not described.

4 Materials and methods

In February 2015, sediment cores were collected at three locations from Lake Tokotan when it was frozen (Fig. 1d). Holes that were approximately 10 cm in diameter were drilled through the ice so that either a 3-m-long handy geoslicer, consisting of a sample tray and a shutter plate driven by a weighted vibrator (Nakata and Shimazaki 1997), or a gravity corer can sample the lake sediment. At location 1 (1.8 m water depth), samples were retrieved using a handy geoslicer (3 m long and 10 cm wide) and a gravity core sampler (1 m long and 8 cm diameter). Six geoslicer samples were collected for observation and analyses. Short cores (about 20 cm long) were taken at locations 2 (1.5 m water depth) and 3 (1.5 m water depth) so that correlations could be made among the three sites. Regarding the core sediments, it was not possible to photograph the entire core or make a peel because the core sample consisted of soft mud. Therefore, it could not lean. Core samples were stored in a vertical position following extraction to prevent outflow of the soft surface mud.

Descriptions and analyses of the stratigraphic layers were conducted of two sliced samples (Slices 1A and 1B) that had been collected at the same location to avoid any chemical contamination resulting from the glue used to create peels. Different analyses were conducted between slice and core samples (Table 2). The sliced samples from location 1 were first described stratigraphically in the field. Later, they were peeled using hydrophilic glue (SAC-100) to observe detailed sedimentary structures by topographic relief, which highlights bedding defined by grain size differences. The sliced samples were also observed using soft X-ray tomography. Other samples from locations 2 and 3 were observed using 3D imaging based on X-ray computed tomography (CT) (LightSpeed Ultra 16; GE Healthcare Japan) at the Center for Advanced Marine Core Research, Kochi University. Volcanic ash layers within the slice were identified stratigraphically based on color and size (ash or pumice) related to previous studies (Tokui 1989; Furukawa et al. 1997). Tephra samples were rinsed with water for 30 min using an ultrasonic generator. The major elemental composition of volcanic glass was analyzed using energy-dispersive X-ray spectrometry.

For core sediment analysis, 0.5–1.0 cm intervals were subsampled. To calculate sand content (weight %), subsamples were sieved at 63 μm (4 phi) to remove the mud fraction. Grain size analysis was performed on the residual sand samples using an image analyzer (Camsizer, Retsch Technology GmbH, Haan, Germany) with an effective measuring range

Table 2 Analyses conducted of each sample

	Core sample	Slice 1A	Slice 1B
Photograph		✓	
Peel			✓
Soft X-ray image			✓
CT	✓	✓	
Cs and Pb radioisotopes	✓	✓	
Grain size	✓		
Ions		✓	

of -5.25 phi (pebble) to 6.25 phi (silt) at intervals of 0.25 phi. Before analysis, organic matter was removed from subsamples using a 30% hydrogen peroxide solution for 24 h. Then, each sample was then dried at 60 °C for 24 h.

Measurements of radioactive cesium and lead were taken of 1.5–3.0 g samples using a gamma spectrometer (GCW2022; Canberra Industries Inc., USA) at 2 cm resolution. The ^{137}Cs ($T_{1/2} = 30.2$ years) or ^{210}Pb ($T_{1/2} = 22.2$ years) data are used for dating the recent deposit during the last several tens of years to one hundred years (e.g., He and Walling 1997; Wren and Davidson 2011). The excess ^{210}Pb was calculated to exclude ^{214}Pb that is under radioactive equilibrium from ^{210}Pb. The concentration of ^{134}Cs ($T_{1/2} = 2.06$ years) was nearly below the limit of detection throughout the core samples. Water-leachable ions were measured in sliced samples following the methods described by Chagué-Goff et al. (2012). Water-leachable cations (Na^+, Mg^{2+}, Ca^{2+}, K^+, Mn^{2+}, and Sr^{2+}) were elucidated using inductively coupled plasma-atomic emission spectroscopy (ICP-AES, SPS3500DD; Seiko Instruments Inc., Japan), while water-leachable anions (Cl^-, SO_4^{2-}, Br^-, NO_3^-, F^-, and PO_4^{3-}) were measured using ion chromatography (IC-2001; TOSOH CO., Japan).

5 Results

5.1 Lithostratigraphy and geochemistry

5.1.1 Location 1

A 75-cm-long sliced sample (Slice 1) was obtained at location 1 using a geoslicer (Fig. 1d). The sediment consists mainly of black organic-rich mud, sand, and volcanic ash. Three faint sandy layers (E1, E2, and E3) were observed within the black mud using soft X-ray imaging (Fig. 2). Several centimeters below the faint sandy layers, a 1-cm-thick sand layer (E4) was observed with a sharp lower stratigraphic contact by visual observation. Below E4, three tephra layers (T1, T2, and T3) were intercalated with mud (Fig. 2). At 40 cm deep from the top of the slice, another sand layer (E5) was present. The E5 layer consists of a lower sand and upper muddy sand subunits. The lower sand layer was visible by unassisted visual observation, but it was thin. The upper muddy layer was difficult to recognize using unassisted visual observation alone, but it was detected easily in the soft X-ray image. At 46–67 cm deep, alternation of sand and peat layers was recognized. At this stage, it is difficult to ascertain whether the sand layers represent a few small events that occurred very close in time, or the repetition of large waves during one event. This study tentatively interprets the sandy layers as a single event. The thick sandy unit (E6) has sharp lower and upper stratigraphic contacts with organic mud. In the E6 sand layer, parallel laminations were observed within the sand layers. Angular gravels were found in the lower part of the unit (Fig. 2). Below E6, a 3-cm-thick sand layer (E7) was intercalated with a mud deposit.

In the 20-cm-long core sample obtained using the gravity corer at location 1, three sand layers are also recognizable using CT image and grain size analyses (Figs. 3a and 4a). At the muddy layer, the sand content and mean grain size for the sand fraction were, respectively, ca. 5% and ca. 3.0 phi, although they were 7–71% and 1.8–2.2 phi at the three sand layers (Fig. 3a). The sand fraction within the muddy layer was well sorted. The grain size range was about 2–4 phi (Fig. 4a). Within the uppermost and middle sand layers, sands were poorly sorted. The ranges were 1–4 phi (Fig. 4a). At the lowermost
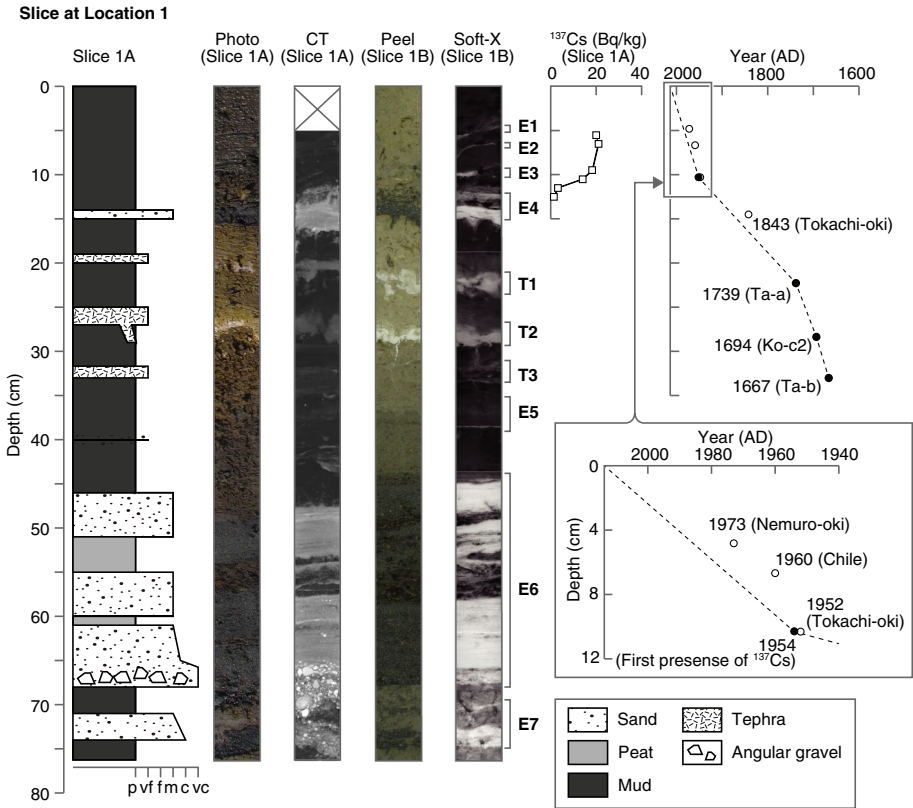
Fig. 2 Lithologic profile at location 1 collected using a handy geoslicer. Stratigraphy, photography, CT image, peel, soft X-ray image, profile of ^{137}Cs, and sedimentation curve are shown. Stratigraphy is based on unassisted visual observation. In the CT image, the upper 5 cm is absent because the surface sediment of the Slice 1A was sampled for the sample bag as a whole. A few tens of centimeters were lost during sample retrieval. Therefore, the zero on the vertical axis does not represent the actual lake bottom

sand layer, although sand was poorly sorted (1–4 phi) at the upper part, it was relatively well sorted (1–3 phi) at a lower part of the sand layer.

Three volcanic ash layers (T1, T2, and T3) were identified within the slice sample (Fig. 2). Sawai (2002) reported that volcanic ash layers derived from the eruptions of Mt. Tarumai (Fig. 1b) in 1739 and 1667 (Ta-a and Ta-b, respectively) and Mt. Komagatake (Fig. 1b) in 1694 (Ko-c2) are present within the Lake Tokotan stratigraphy. Major elements, especially K_2O and TiO_2, are useful to discriminate these ash layers based on their composition (Tokui 1989; Furukawa et al. 1997). The K_2O and TiO_2 contents of each sampled volcanic glass shard are presented in Fig. 5. Actually, T1 and T3 plotted within the range of past Mt. Tarumai eruptions, whereas T2 plotted within the range of past Mt. Komagatake eruptions. Based on their stratigraphic position and results from major elements, T1, T2, and T3 were correlated, respectively, with Ta-a, Ko-c2, and Ta-b.

The concentration of ^{137}Cs ($T_{1/2} = 30.1$ years) varied throughout the core (Fig. 3a). It was ca. 22 Bq/kg at 0–15 cm depth in Core 1, but it decreased gradually with depth, reaching almost 0 Bq/kg at a depth of 20 cm. The variation in concentration of excess ^{210}Pb and
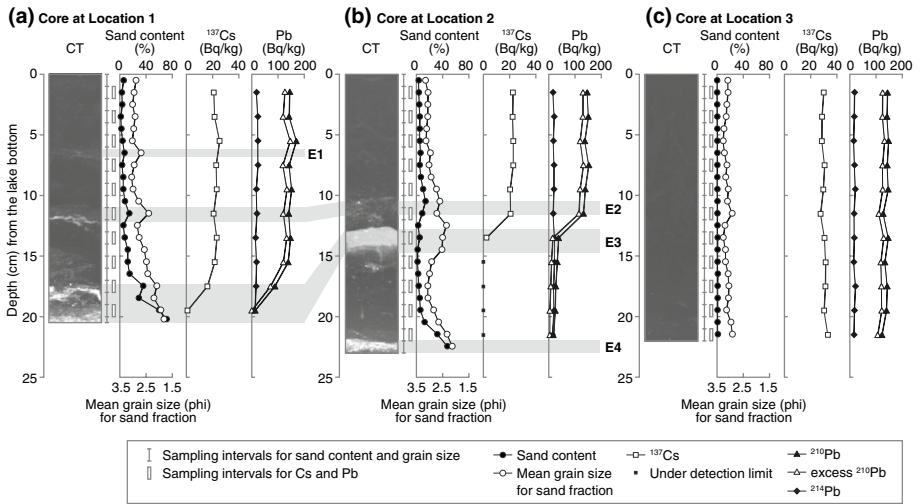
Fig. 3 CT images and depth profiles of sand content, mean grain size, and cesium and lead concentrations for cores collected at **a** location 1, **b** location 2, and **c** location 3 using a gravity corer. Black squares denote values below the detection limit
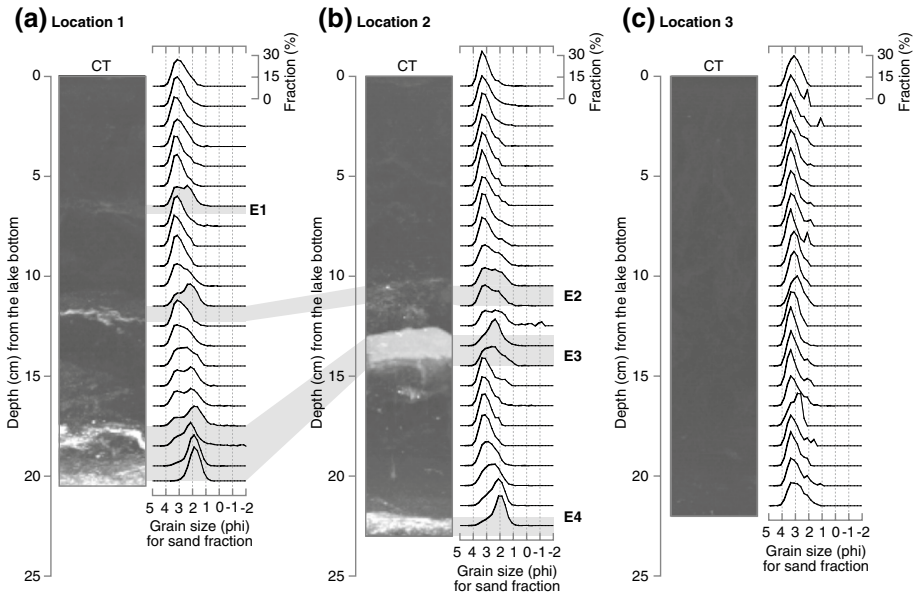

Fig. 4 CT images and vertical changes in grain size distribution for cores collected using a gravity corer at **a** location 1, **b** location 2, and **c** location 3
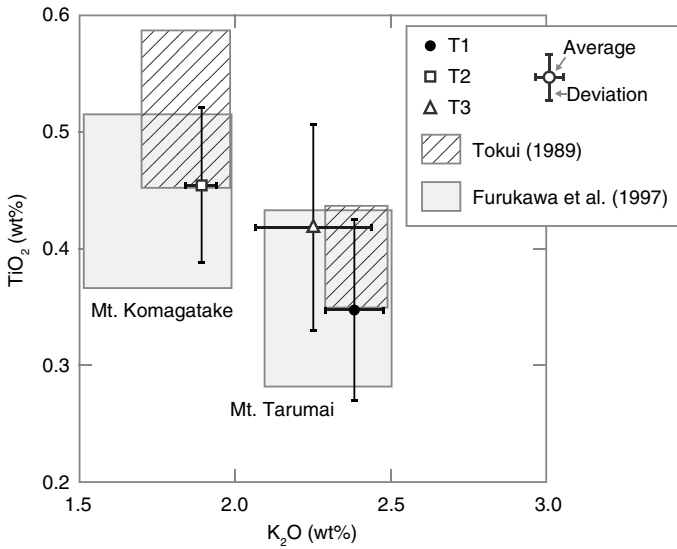
Fig. 5 K_2O and TiO_2 content of each volcanic glass shard from the T1, T2, and T3 tephra layers in the slice sample. Rectangles show the range in elemental concentration of known volcanic ash layer as documented by Tokui (1989) and Furukawa et al. (1997)

^{210}Pb was almost equal to that of ^{137}Cs (Fig. 3a). However, ^{214}Pb was approximately constant (10–20 Bq/kg) at all core depths (Fig. 3a).

In Slice 1, the ^{137}Cs concentration was ca. 20 Bq/kg within the mud layer above E4, but it decreased to almost 0 Bq/kg at the upper part of the sand layer (Fig. 2). The values and curves were similar to those found from core samples collected at the same location (Fig. 3a).

Water-leachable ions were measured at every 0.5 cm interval above E4 in Slice 1 (Fig. 6). Concentration profiles of sodium, magnesium, calcium, manganese, and strontium showed similar variations. They were approximately constant within the mud layer but decreased at ca. 10 cm deep. In addition, only manganese had a low peak at 4 cm deep. The potassium concentration fluctuated. It had two peaks at 4 cm and 6 cm deep. The potassium concentration was extremely low just above E4.

The chloride concentration remained mostly constant throughout the mud layer, except for an interval of 7–8 cm deep (Fig. 6). The fluoride concentration increased with depth with little fluctuation. The nitrogen dioxide concentration peaked at 1–2 cm deep at which point it decreased with depth. The sulfate concentration showed little fluctuation between 0 and 7 cm deep, but it fluctuated noticeably at 7–12 cm deep.

5.1.2 Location 2

Sediment samples from location 2 consist mainly of black organic-rich mud (Fig. 3b). The black mud contains three faint sandy layers. The three layers are not easily discernable with the naked eye, but they are recognizable by CT images and grain size analyses (Figs. 3b and 4b). Within the muddy layer, the sand content and mean grain size for the sand fraction were ca. 5% and ca. 3.0 phi, respectively, whereas they were 5–50% and 2.1–2.7 phi at three sand layers (Fig. 3b). The sand fraction within the muddy layer was well sorted. The
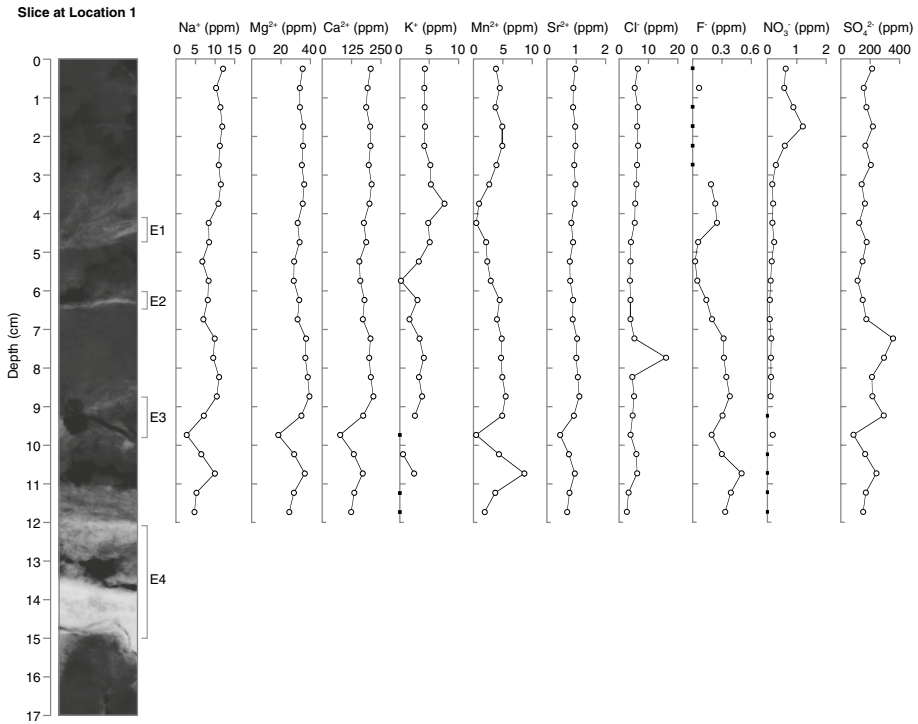
Fig. 6 Soft X-ray image and depth profiles of water-leachable ions of the slice collected at location 1. Black squares denote values below the detection limit

range was about 2–4 phi, although the fractions were poorly sorted, with ranges of 1–4 phi at three sand layers (Fig. 4b).

The ^{137}Cs concentration was ca. 22 Bq/kg at 0–12 cm depth. It decreased to almost 0 Bq/kg at 14 cm depth. It was below the detection limit at further deeper layers in Core 2 (Fig. 3b). The variations in concentration of excess ^{210}Pb and ^{210}Pb were almost identical to that of ^{137}Cs (Fig. 3b). However, ^{214}Pb was relatively constant (10–20 Bq/kg) at all core depths (Fig. 3b).

5.1.3 Location 3

Sediment samples from location 3 consist of black organic-rich mud (Fig. 3c). The black mud includes no significant layers that might be detected from CT images and grain size analyses (Figs. 3c and 4c), with the sand content remaining at almost zero from the top to the bottom of the core. The mean grain size for the sand fraction of the core was 2.9–3.2 phi. The grain size distribution was within the range of 2–4 phi. It sometimes showed spikes (Fig. 4c).

The ^{137}Cs concentration was ca. 30 Bq/kg throughout Core 3. The variation in concentrations of excess ^{210}Pb and ^{210}Pb was almost identical to that of ^{137}Cs in every sample (Fig. 3c). However, ^{214}Pb was constant (10–20 Bq/kg) throughout all core samples (Fig. 3c).

6 Discussion

6.1 Stratigraphic correlation

The ^{137}Cs concentrations allow for stratigraphic correlations among the three sampled locations. Depletion of the ^{137}Cs concentration was observed around the sand layers in both locations 1 and 2 (Figs. 2 and 3). Variations within the ^{137}Cs concentration throughout each core reveal that the E3 sand layer from Slice 1 (Fig. 2) can be correlated to the basal sand layer of the location 1 core (Fig. 3a) and to the middle sand layer of core at location 2 (Fig. 3b). The upper two sand layers observed from the core at location 1 correlate stratigraphically to the E1 and E2 layers. The E1 sand layer was not observed at location 2. In all, four event sand layers (E1–E4) were distinguished from the collected core samples (Fig. 3).

6.2 Origin of faint sand layers

No clear sedimentological structure exists for the faint sandy layers (E1–E3). Rather, this study tested the use of geochemical analyses on water-leachable ions throughout the slice samples from location 1. Marked peaks were observed only at the E3 sand layer (Fig. 6). The concentrations decreased with depth in E3 and increased within the lower mud layer. Similar trends were reported from recent studies conducted in terrestrial environments (e.g., Chagué-Goff et al. 2012; Shinozaki et al. 2016). Although no significant peaks were observed at E1 and E2 sand layers, the results obtained from the E3 sand layer suggest that geochemical analysis might be able to detect faint layers within lake sediment.

Landward fining and thinning of the sand layers at locations 1–3 may suggest that E2 and E3 were likely to be transported from the sea to the lake. Although only three locations were sampled, horizontal profiles of mean grain size show that landward locations have finer event deposits (E2 and E3). Moreover, the sand content decreased at the E2 and E3 layers from locations 1 and 2 (Fig. 3). Grain size distributions also represent a trend of landward fining in the E2 and E3 layers (Fig. 4). Although the range of grain size for sand fractions at E2 layer was 1–4 phi at both in locations 1 and 2, the peaks were 2 phi and 3 phi, respectively, at locations 1 and 2, suggesting that relatively finer fraction was dominant at location 2. The E3 layer also represents that the peak was smaller at location 1 than at location 2. These changes show that the distribution of sands E2 and E3 is limited to the seaward and central areas of the lake (Fig. 3). Grain size and thickness of the event deposits are generally variable within a small sedimentary basin (2004 Sumatra tsunami, Matsumoto et al. 2010; 2011 Tohoku tsunami, Szczuciński et al. 2012), but results from our analyses might reflect waning current velocities as fining and decreasing sand contents in a landward direction.

6.3 Correlation with historical and prehistoric tsunami events

Variation within the radioactive concentrations plays a crucially important role in determining the depositional age of these sand layers. The first presence of ^{137}Cs is regarded as 1954 because measurable amounts of ^{137}Cs have generally been identified from sediment (Longmore 1982; Ritchie and McHenry 1990; Appleby 2001). Other significant peaks are those of 1963 and 1986, caused, respectively, by weapon fallout and the Chernobyl reactor incident (Marshall et al. 2007). In the last decades, geology applied the occurrence and

peaks of the radioactive cesium to estimate the recent depositional ages for lakes and coasts (e.g., Simpson et al. 1976; Robbins et al. 1978; Kemp et al. 2013; Tamura et al. 2015; Drexler et al. 2018).

The occurrence of cesium within sediment cores from Lake Tokotan represents the limiting minimum age of the event E3. Profiles of vertical changes in cesium demonstrate that the concentration of ^{137}Cs decreases rapidly. It becomes almost zero within the E3 layer at location 2, whereas cesium was present within the uppermost part of the E3 layer at location 1 (Fig. 3). The presence of cesium within the uppermost part of E3 is likely to be attributable to the subsample inclusion of some portion of mud above the E3 layer. However, the pronounced ^{137}Cs peaks of 1963 and 1986 were not observed at every location (Fig. 3). Such ambiguous peaks in the cesium profile are producible by vertical mixing of the deposits, mainly because of bioturbation. However, optical observations by CT images revealed stratigraphic sharp contacts and no clear presence of biogenic disturbance. A potential reason for the lack of clear cesium peaks might be the holomictic or dimictic environments in the lake because it freezes during the winter months. If this is the case, then freezing will cause vertical mixing of the ^{137}Cs within the lake water before settling of ^{137}Cs with fine mud fractions. Consequently, the vertical distribution of the ^{137}Cs becomes peakless. We were unable to identify the horizons associated with the two ^{137}Cs peaks, where ^{137}Cs was first recognized as limiting minimum age.

Appearance of ^{137}Cs just above the E3 layer at locations 1 and 2 suggests that the E3 layer is predated to at least 1954 as the onset date of ^{137}Cs. Historical tsunamis reported before 1954 were the 1952 Tokachi-oki tsunami and the 1843 Tokachi-oki tsunami (Table 1). Considering the sedimentation rate, the E3 layer would be correlated with the 1952 Tokachi-oki tsunami.

Given the sedimentation rate and the history of tsunamis and storms at this location, the candidate events for the two younger layers (E1 and E2) are probably the 1973 Nemuro-oki and 1960 Chilean tsunamis. The E4 layer just below E3 might be correlated with the 1843 Tokachi-oki tsunami, shown as the youngest event deposit in Shigeno et al. (2007). The 1879 storm recorded at Akkeshi Town is another potential candidate that might have deposited the E4 layer. However, the 1879 storm is unlikely to leave a substantial sand layer because the corresponding storm waves were smaller than the twentieth and twenty-first century tsunamis.

We were not able to recognize the tsunami deposit associated with the 2003 event. In the 2003 event, the tsunami waves were 1.9 m to 3.1 m high and might have run up along the drainage river from the sea and might have intruded into the lake. A faint event deposit could have been deposited toward the top of the core if this scenario were to happen. However, this study revealed no candidates for the 2003 event using CT and soft X-ray images. The 2003 tsunami was apparently comparable in wave height to the other historical tsunamis (Table 1). One reason for the absence of deposits from the 2003 tsunami is that the tide was lower during the tsunami. In fact, the tide was decreasing at the time of the earthquake occurred (Hirata et al. 2004), resulting in tsunami waves that were not sufficient to inundate and transport sediment into the lake. Alternatively, the lack of a deposit associated with the 2003 tsunami might simply be the result of a disturbance of the lake floor during sample collection.

The deeper event deposits are correlatable with prehistoric tsunami deposits described by previous studies. The CT and soft X-ray images recognized a thin sand layer with overlying laminated mud (E5) immediately below the Ta-b tephra. Based on the sand layer position relative to the Ta-b tephra (1667 CE), the event E5 is correlated with the latest multi-segment earthquake, which is regarded as having occurred in the seventeenth century

(KS3 in Nanayama et al. 2007, K2 and MP2 in Sawai et al. 2009). Events deeper than the E5 layer are likely to be correlated with older events (probably the thirteenth and tenth century tsunamis; Nanayama et al. 2007), but the lack of radiocarbon ages limits any further correlations.

As shown in previous studies, events older than the Ta-b tephra were unusually large by comparison with recent tsunamis (Nanayama et al. 2003). According to documented records by research groups, tsunami waves in 1973 reached more than approximately 2 m above sea level and ran inland along the Tokotan River (see study area, Fig. 1d) (Bureau for Ports and Harbours et al. 1973). The run-up current probably eroded the river bottom, transporting the coarse particles, and redepositing them mainly around the river entrance. Considering the height of the sand barrier along the coast as well as the wave heights in 1960 (less than 2 m at Tokotan), the 1960 Chilean tsunami waves inundated the lake through the floor of the Tokotan River and were accompanied by coarse sediments. In contrast, events older than Ta-b show widespread distribution within Lake Tokotan (Nanayama et al. 1998; Sawai 2002; Shigeno et al. 2007). Although there might be topographic difference, such as the position of the shoreline or dune height, between thirteenth century and today, event deposits older than Ta-b show that widespread distribution is likely because the older tsunamis had high-energy currents with sufficient capacity to erode and transport sand particles from the coast into the furthest reaches of the lake.

7 Conclusion

Evidence for small tsunamis can be lost easily or can be obscured by post-depositional changes, making them difficult to detect using the naked eye. Nevertheless, nondestructive techniques and radionuclide analysis can facilitate the detection of heretofore invisible tsunami deposits within unstructured sediment samples. Results of this study revealed a set of three faint sand layers that can be correlated with the 1973 Nemuro-oki, 1960 Chilean, and 1952 Tokachi-oki tsunamis that struck eastern Hokkaido. This combined analytical technique is applicable to similar geological contexts for identifying smaller tsunamis that have left only faint depositional evidence.

References

Akkeshi Town (2007) Akkeshi Cho Shi. Gyousei Co., Ltd., Hokkaido, p 839 (in Japanese)
Akkeshi Town (2015) Shin Akkeshi Cho Shi. Shiryou Hen 2. Nikkanki. Gyousei Co., Ltd., Tokyo, p 1007 (in Japanese)
Appleby PG (2001) Chronostratigraphic techniques in recent sediment. In: Last WM, Smol JP (eds) Tracking environmental change using lake sediments basin analysis 1 coring and chronological techniques. Springer, Berlin, pp 171–203
Barrientos SE, Ward SN (1990) The 1960 Chile earthquake: inversion for slip distribution from surface deformation. Geophys J Int 103(3):589–598

Bureau for Ports and Harbours (Ministry of Transport), Port and Harbour Research Institute (Ministry of Transport), and Port and Harbour Division (Hokkaido Development Bureau, Hokkaido Development Agency) (1973) The report on the damage to port structures and the investigation of the tsunami caused by the Nemuro Hanto oki earthquake on June 17, 1973. Ministry of Transport, Tokyo, p 139

Central Meteorological Agency (1953) Reports of the Tokachi-oki earthquake of March 4, 1952. Q J Seismol 17:1–135

Chagué-Goff C, Niedzielski P, Wong HKY, Szczuciński W, Sugawara D, Goff J (2012) Environmental impact assessment of the 2011 Tohoku-oki tsunami on the Sendai Plain. Sediment Geol 282:175–187

Cisternas M, Atwater BF, Torrejón F, Sawai Y, Machuca G, Lagos M, Eipert A, Youlton C, Salgado I, Kamataki T, Shishikura M, Rajendran CP, Malik JK, Rizal Y, Husni M (2005) Predecessors of the giant 1960 Chile earthquake. Nature 437:404–407

Drexler JZ, Fuller CC, Archfield S (2018) The approaching obsolescence of ^{137}Cs dating of wetland soils in North America. Quaternary Sci Rev 199:83–96

Elsner JB, Liu KB (2003) Examining the ENSO–typhoon hypothesis. Climate Res 25:43–54

Fujino S, Naruse H, Matsumoto D, Jarupongsakul T, Sphawajruksakul A, Sakakura N (2009) Stratigraphic evidence for pre-2004 tsunamis in southwestern Thailand. Mar Geol 262:25–28

Furukawa R, Yoshimoto M, Yamagata K, Wada K, Ui T (1997) Did Hokkaido Komagatake volcano erupt in 1694?: Reappraisal of the eruptive ages of 17–18th centuries in Hokkaido. Kazan 42:269–279 **(in Japanese with English abstract)**

Goff J, Chagué-Goff C, Nichol S, Jaffe B, Dominey-Howes D (2012) Progress in palaeotsunami research. Sediment Geol 243–244:70–88

Goto K, Chagué-Goff C, Fujino S, Goff J, Jaffe B, Nishimura Y, Richmond B, Sugawara D, Szczuciński W, Tappin DR, Witter RC, Yulianto E (2011) New insights of tsunami hazard from the 2011 Tohoku-oki event. Mar Geol 290:46–50

Hatori T (1984) Source area of the east Hokkaido tsunami generated in April, 1843. Bull Earthq Res Inst Tokyo 59:423–431 **(in Japanese with English abstract)**

He Q, Walling DE (1997) The distribution of fallout ^{137}Cs and ^{210}Pb in undisturbed and cultivated soils. Appl Radiat Isot 48(5):677–690

Hirata K, Tanioka Y, Satake K, Yamaki S, Geist EL (2004) The tsunami source area of the 2003 Tokachi-oki earthquake estimated from tsunami travel times and its relationship to the 1952 Tokachi-oki earthquake. Earth Planets Space 56:367–372

Ioki K, Tanioka Y (2016) Re-estimated fault model of the 17th century great earthquake off Hokkaido using tsunami deposit data. Earth Planet Sc Lett 433:133–138

Inoue U (1954) The Tokachi earthquake of March 4, 1952. In: Mizoguchi Y, Ono K (eds) Report on the Tokachi Oki Earthquake Hokkaido, Japan, March 4, 1952. Special committee for the investigation of the Tokachi-Oki earthquake, Sapporo, pp 1–150 **(in Japanese)**

Jankaew K, Atwater BF, Sawai Y, Choowong M, Charoentitirat T, Martin ME, Prendergast A (2008) Medieval forewarning of the 2004 Indian Ocean tsunami in Thailand. Nature 455:1228–1231

Kemp AC, Horton BP, Vane CH, Bernhardt CE, Corbett DR, Engelhart SE, Anisfeld SC, Parnell AC, Cahill N (2013) Sea-level change during the last 2500 years in New Jersey, USA. Quaternary Sci Rev 81:90–104

Longmore ME (1982) The Caesium dating technique and associated applications in Australia: a review. In: Ambrose W, Duerden P (eds) Archaeometry: an australian perspective. ANU Press, Canberra, pp 310–321

MacInnes BT, Weiss R, Bourgeois J, Pinegina TK (2010) Slip distribution of the 1952 Kamchatka Great Earthquake based on near-field tsunami deposits and historical records. Bull Seismol Soc Am 100(4):1695–1709

Marshall WA, Gehrels WR, Garnett MH, Freeman SPHT, Maden C, Xu S (2007) The use of 'bomb spike' calibration and high-precision AMS ^{14}C analyses to date salt-marsh sediments deposited during the past three centuries. Quaternary Res 68:325–337

Matsumoto D, Shimamoto T, Hirose T, Gunatilake J, Wickramasooriya A, DeLile J, Young S, Rathnayake C, Ranasooriya J, Murayama M (2010) Thickness and grain-size distribution of the 2004 Indian Ocean tsunami deposits in Periya Kalapuwa Lagoon, eastern Sri Lanka. Sediment Geol 230:95–104

Nakanishi A, Smith AJ, Miura S, Tsuru T, Kodaira S, Obana K, Takahashi N, Cummins PR, Kaneda Y (2004) Structural factors controlling the coseismic rupture zone of the 1973 Nemuro-Oki earthquake, the southern Kuril Trench seismogenic zone. J Geophys Res 109:B05305

Nakata T, Shimazaki K (1997) Geo-slicer, a newly invented soil sampler, for high-resolution active fault studies. J Geogr (Chigaku zassi) 106:59–69 **(in Japanese with English abstract)**

Nanayama F (1998) Preliminary study of tsunami deposits along the Pacific coast of eastern Hokkaido. In: Sugiyama Y (ed) Interim report on active faults and paleoearthquake researches in the 1997 fiscal year. EQ/00/2, pp 1–9 (in Japanese with English abstract)

Nanayama F, Shigeno K, Makino A, Satake K, Furukawa R (2001) Evaluation of tsunami inundation limits from distribution of tsunami event deposits along the Kuril subduction zone, eastern Hokkaido, northern Japan: case studies of Lake Choboshi-ko, Lake Tokotan-numa, Lake Pashukuru-numa, Kinashibetsu Marsh and Lake Yudo-numa. Annu Rep Active Fault Paleoearthquake Res 1:251–272 **(in Japanese with English abstract)**

Nanayama F, Satake K, Furukawa R, Shimokawa K, Atwater BF, Shigeno K, Yamaki S (2003) Unusually large earthquakes inferred from tsunami deposits along the Kuril trench. Nature 424:660–663

Nanayama F, Furukawa R, Shigeno K, Makino A, Soeda Y, Igarashi Y (2007) Nine unusually large tsunami deposits from the past 4000 years at Kiritappu marsh along the southern Kuril Trench. Sediment Geol 200(3–4):275–294

Nishimura Y, Miyaji N, Yoshida M, Murata T, Nakagawa M (2000) The 1843 tsunami deposits found in the peat deposit at Kiritappu marsh, eastern Hokkaido, Japan. Quat Res (Daiyonki-Kenkyu) 39(5):451–460 **(in Japanese with English abstract)**

Okumura K (1996) Tephrochronology, correlation, and deformation of marine terraces in eastern Hokkaido, Japan. Geogr Rep Tokyo Metrop Univ 31:19–26

Ritchie JC, McHenry JR (1990) Application of radioactive fallout Cesium-137 for measuring soil erosion and sediment accumulation rates and patterns: a review. J Environ Qual 19:215–233

Robbins JA, Edgington DN, Kemp ALW (1978) Comparative ^{210}Pb, ^{137}Cs, and pollen geochronology of sediments from Lakes Ontario and Erie. Quat Res 10:256–278

Sapporo District Central Meteorological Observatory (1954) Report of the field investigation. (Part of Hokkaido). In: The Special Committee for the Investigation of the TOKACHI-OKI Earthquake (ed) Report on the Tokachi-oki Earthquake, Sapporo, pp 50–103

Saruwatari A, de Lima AC, Kato M, Nikawa O, Watanabe Y (2015) Report on the 2014 winter cyclone storm surge in Nemuro, Japan. Coastal Eng J 57(3):1550014

Satake K, Nanayama E, Yamaki S (2008) Fault models of unusual tsunami in the 17th century along the Kuril trench. Earth Planets Space 60:1–11

Sawai Y (2002) Evidence for 17th-century tsunamis generated on the Kuril-Kamchatka subduction zone, Lake Tokotan, Hokkaido, Japan. J Asian Earth Sci 20:903–911

Sawai Y, Kamataki T, Shishikura M, Nasu H, Okamura Y, Satake K, Thomson KH, Matsumoto D, Fujii Y, Komatsubara J, Aung TT (2009) Aperiodic recurrence of geologically recorded tsunamis during the past 5500 years in eastern Hokkaido Japan. J Geophy Res-Sol Ea 114:B01319. https://doi.org/10.1029/2007JB005503

Sawai Y, Namegaya Y, Okamura Y, Satake K, Shishikura M (2012) Challenges of anticipating the 2011 Tohoku earthquake and tsunami using coastal geology. Geophys Res Lett 39:L21309. https://doi.org/10.1029/2012GL05369

Shigeno K, Nanayama F, Furukawa R, Soeda Y, Kumasaki N (2007) Tsunami traces of the 1843 tsunami and prehistorical three large tsunamis in the lacustrine cores at Tokotan-numa, eastern Hokkaido. In: Abstract of the 114th annual meeting of the geological society of Japan, Hokkaido University, Japan, 9–11 Sept 2007

Shinozaki T, Sawai Y, Hara J, Ikehara M, Matsumoto D, Tanigawa K (2016) Geochemical characteristics of deposits from the 2011 Tohoku-oki tsunami at Hasunuma, Kujukuri coastal plain, Japan. Isl Arc 25:350–368

Simpson HJ, Olsen CR, Trier RM, Williams SC (1976) Man-made radionuclides and sedimentation in the Hudson River estuary. Science 194:179–183

Szczuciński W, Kokociński M, Rzeszewski M, Chagué-Goff C, Cachão M, Goto K, Sugawara D (2012) Sediment sources and sedimentation processes of 2011 Tohoku-oki tsunami deposits on the Sendai Plain, Japan—insights from diatoms, nannoliths and grain size distribution. Sediment Geol 282:40–56

Tamura T, Sawai Y, Ikehara K, Nakashima R, Hara J, Kanai Y (2015) Shallow-marine deposits associated with the 2011 Tohoku-oki tsunami in Sendai Bay, Japan. J Quaternary Sci 30:293–297

Tanioka Y, Nishimura Y, Hirakawa K, Imamura F, Abe I, Abe Y, Shindou K, Matsutomi H, Takahashi T, Imai K, Harada K, Namegawa Y, Hasegawa Y, Hayashi Y, Nanayama F, Kamataki T, Kawata Y, Fukasawa Y, Koshimura S, Hada Y, Azumai Y, Hirata K, Kamikawa A, Yoshikawa A, Shiga T, Kobayashi M, Masaka S (2004) Tsunami run-up heights of the 2003 Tokachi-oki earthquake. Earth Planets Space 56:359–365

The Committee for field investigation of the Chilean tsunami of 1960 (1961) Report on the Chilean tsunami of May 24, 1960, as observed along the coast of Japan. Maruzen Co., Ltd., Tokyo, p 397

The Japan Meteorological Agency (1961) Report on the tsunami of the Chilean earthquake. Technical Report of the Japan Meteorological Agency, 8, The Japan Meteorological Agency, Tokyo, p 389 (in Japanese)

The Japan Meteorological Agency (1974) Report on the Nemuro-Hanto-oki earthquake of June 17, 1973. Technical Report of the Japan Meteorological Agency, 87, The Japan Meteorological Agency, Tokyo, p 102 (in Japanese)

Tokui Y (1989) Volcanic eruptions and their effects on human activity, in Hokkaido, Japan. Ann Ochano-mizu Geogr Soc 30:27–33 **(in Japanese)**

Utsu T (1999) Seismicity Studies: A Comprehensive Review. Univ of Tokyo Press, Tokyo, p 876 (in Japanese)

Watanabe H (1998) Comprehensive list of tsunamis to hit the Japanese islands [second edition]. University of Tokyo Press, Tokyo, p 238

Wren DG, Davidson GR (2011) Using lake sedimentation rates to quantify the effectiveness of erosion control in watersheds. J Soil Water Conserv 66(5):313–322

Yamanaka K, Kikuchi M (2003) Source processes of the Tokachi-oki earthquake on September 26, 2003 inferred from teleseismic body waves. Earth Planets Space 55:e21–e24